

VISAGG

Visualization and Graphics Group



UNIVERSITY OF
CALGARY

Rendering in Shift-Invariant Spaces

Usman R. Alim

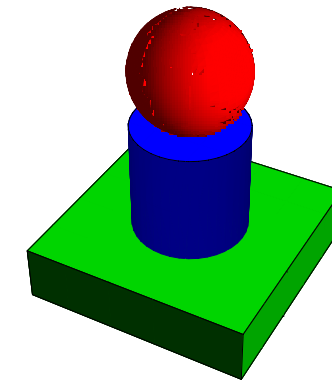
Department of Computer Science
University of Calgary

May 31, 2013

Motivation

- Image function describes a continuous 2D image.

$$f : \mathbb{R}^2 \rightarrow \mathbb{R}$$



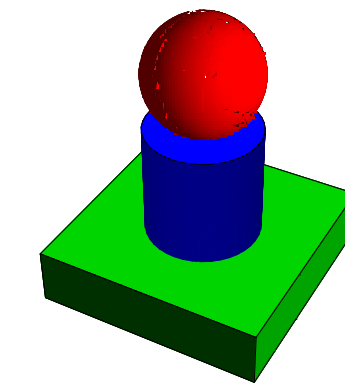
continuous 2D image

Motivation

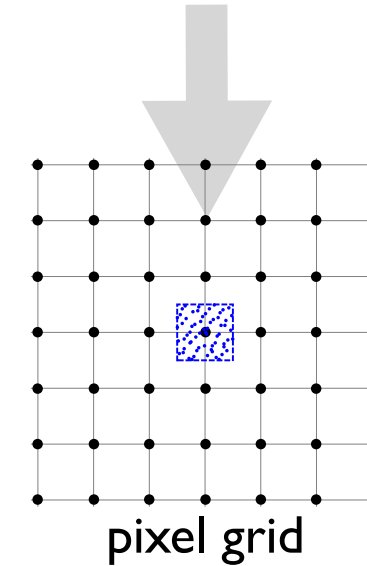
- Image function describes a continuous 2D image.

$$f : \mathbb{R}^2 \rightarrow \mathbb{R}$$

- In rendering, we typically use *area sampling* to discretize the image function f .



continuous 2D image



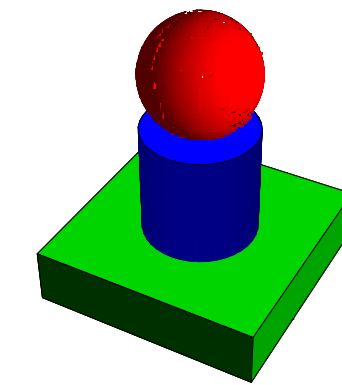
pixel grid

Motivation

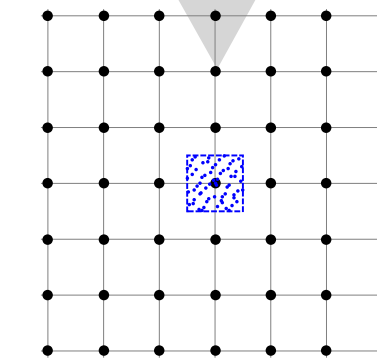
- Image function describes a continuous 2D image.

$$f : \mathbb{R}^2 \rightarrow \mathbb{R}$$

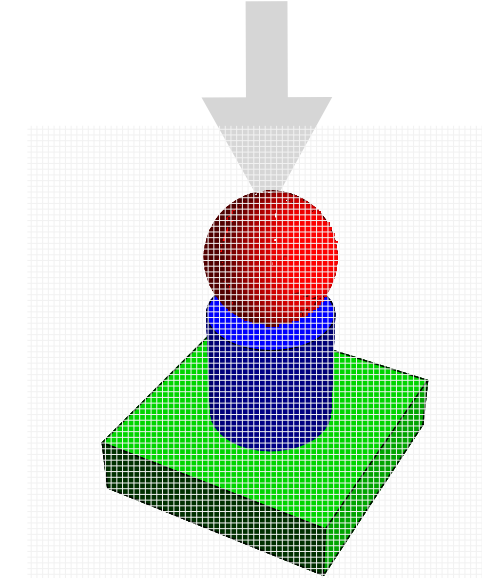
- In rendering, we typically use *area sampling* to discretize the image function f .
- This yields a discrete approximation of f .
(can be regarded as continuous in light of Shannon's sampling theory)



continuous 2D image



pixel grid



discrete approximation

Goals

- Use recent developments in signal processing and approximation theory to seek higher-quality grid-based approximations.
- Approximate f in a *shift-invariant space*.
- Seek an approximation f_{app} that minimizes the L_2 error:
$$\|f - f_{\text{app}}\|_{L_2(\mathbb{R}^2)}.$$
- Investigate the quality improvements in the context of ray-tracing.

Outline

- Motivation
- **Shift-Invariant (SI) spaces**
- Rendering in spaces generated by the uniform B-splines
- Results
- Conclusion

Use in Graphics

- More familiar to the image-processing community [[Unser 2000](#)]
- Some recent applications in scientific visualization:
 - volume reconstruction [[Entezari et al. 2008](#)]
 - gradient estimation [[Alim et al. 2010](#)]
- In rendering, antialiasing approaches are largely based on Shannon's sampling theory. SI spaces offer a much more flexible alternative.

Shift-invariant spaces (ID)

- A vector-space spanned by the (scaled) shifts of a generating function:

$$\mathbb{V}(\varphi) := \left\{ g(x) = \sum_{n \in \mathbb{Z}} c[n] \varphi(x - n) : c \in l_2(\mathbb{Z}) \right\}$$

- The sequence $\{\varphi(x - n)\}_{n \in \mathbb{Z}}$ forms a basis for $\mathbb{V}(\varphi)$.
 (The basis may not be orthogonal)

Inner product:

$$\langle f, g \rangle := \int_{\mathbb{R}} f(x)g(x)dx$$

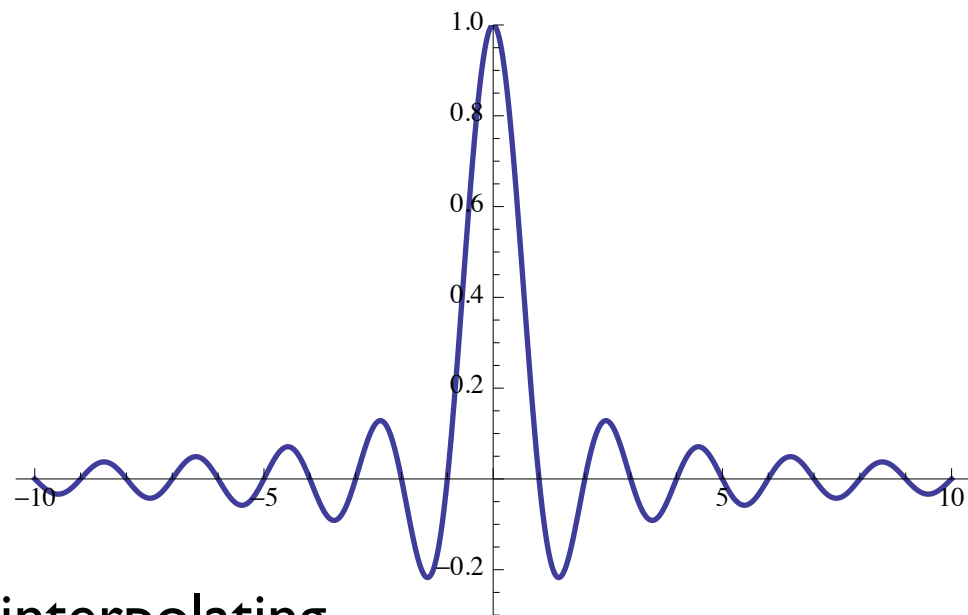
- There exists a *dual basis* $\{\dot{\varphi}(x - n)\}_{n \in \mathbb{Z}}$ that also spans $\mathbb{V}(\varphi)$. Primal and dual generators are bi-orthonormal:

$$\langle \varphi, \dot{\varphi}(\cdot - n) \rangle = \delta[n]$$

Familiar Examples

- Shannon's sampling theory is a special case.

$$\varphi(x) = \text{sinc}(x)$$

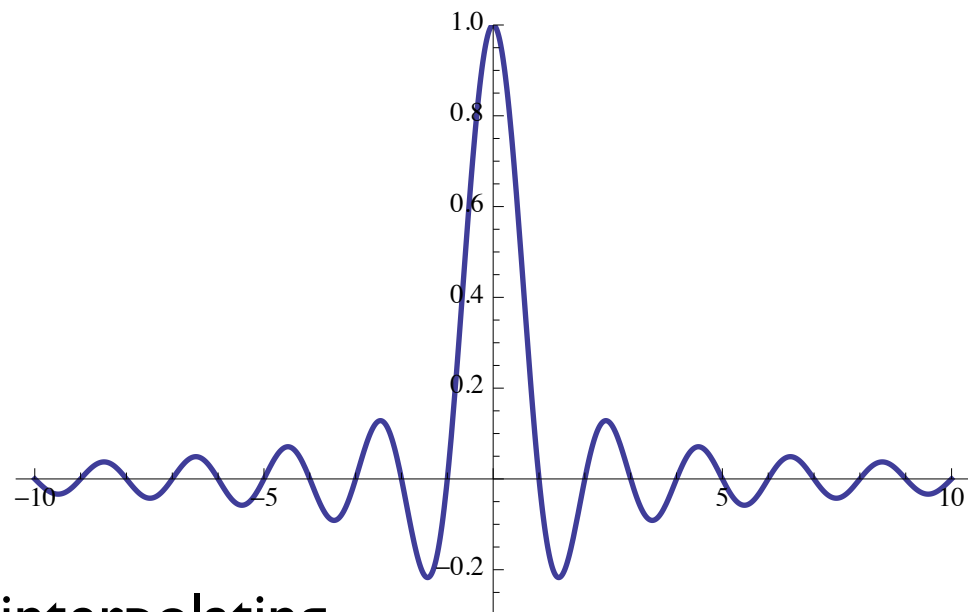


- interpolating
- infinite support (not practical)
- self-dual
- can represent all bandlimited functions

Familiar Examples

- Shannon's sampling theory is a special case.

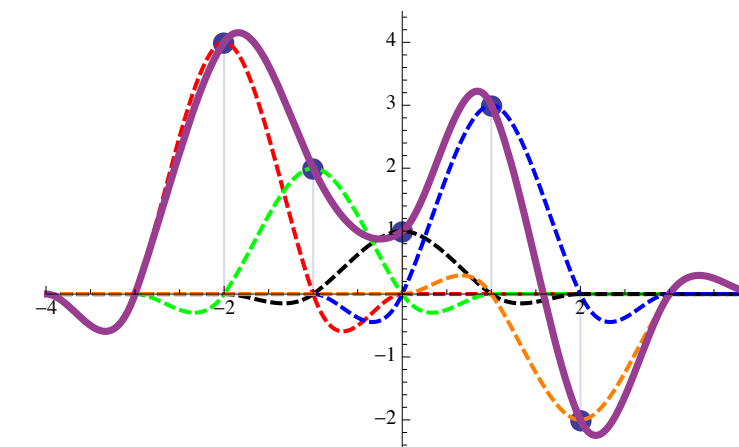
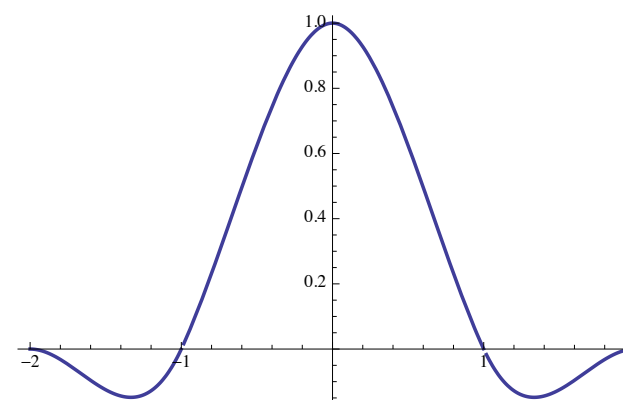
$$\varphi(x) = \text{sinc}(x)$$



- interpolating
- infinite support (not practical)
- self-dual
- can represent all bandlimited functions

- Cubic interpolation [Mitchell Netravali 88]

$$\varphi(x)$$



- interpolating
- compact support (practical)
- primal and dual are piecewise cubic
- can represent all cubic polynomials

Minimum-error Approximation

- Minimum-error approximation is obtained by orthogonally projecting f to the desired space $\mathbb{V}(\varphi)$.

- Image approximation:

$$f_{\text{app}}(x) = \sum_n c[n] \varphi(x - n).$$

- Measure the coefficients according to:

$$c[n] = \langle f, \dot{\varphi}(\cdot - n) \rangle$$

Minimum-error Approximation

- Minimum-error approximation is obtained by orthogonally projecting f to the desired space $\mathbb{V}(\varphi)$.

- Image approximation:

$$f_{\text{app}}(x) = \sum_n c[n] \varphi(x - n).$$

(φ does not need to be an interpolating generator)

- Measure the coefficients according to:

$$c[n] = \langle f, \dot{\varphi}(\cdot - n) \rangle$$

Minimum-error Approximation

- Minimum-error approximation is obtained by orthogonally projecting f to the desired space $\mathbb{V}(\varphi)$.

- Image approximation:

$$f_{\text{app}}(x) = \sum_n c[n] \varphi(x - n).$$

(φ does not need to be an interpolating generator)

- Measure the coefficients according to:

$$c[n] = \langle f, \dot{\varphi}(\cdot - n) \rangle$$

(the dual $\dot{\varphi}$ is usually not compactly supported)

Outline

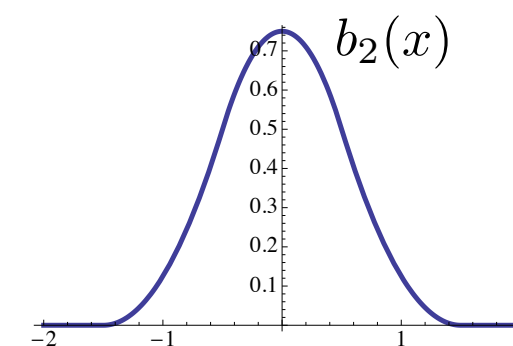
- Motivation
- Shift-Invariant (SI) spaces
- **Rendering in spaces generated by the uniform B-splines**
- Results
- Conclusion

Uniform Centered B-splines

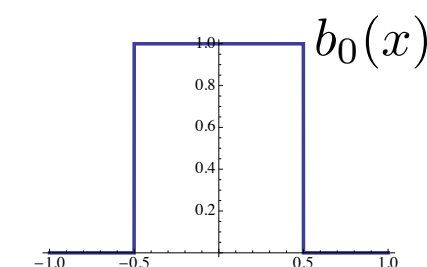
- The uniform centered B-spline $b_d(x)$ (d -degree) is obtained via d convolutions of the box function.

$$\begin{aligned}
 b_d(x) &:= \underbrace{(b * b * \dots * b)}_{d+1 \text{ repetitions of } b}(x) \\
 &= (b * b_{d-1})(x)
 \end{aligned}$$

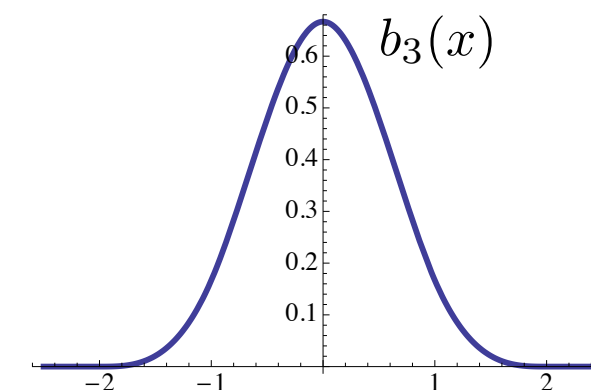
- For example, the cubic B-spline can be obtained in two different ways:



*



=

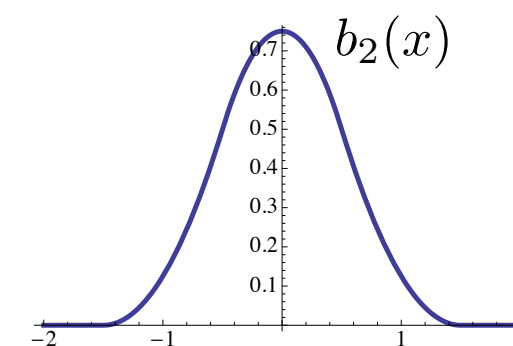


Uniform Centered B-splines

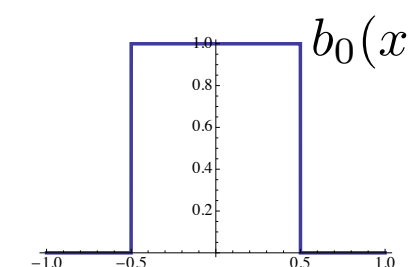
- The uniform centered B-spline $b_d(x)$ (d -degree) is obtained via d convolutions of the box function.

$$b_d(x) := \underbrace{(b * b * \dots * b)}_{d+1 \text{ repetitions of } b}(x)$$

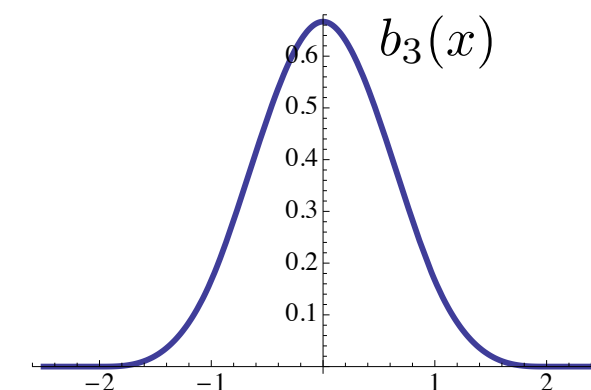
$$= (b * b_{d-1})(x)$$



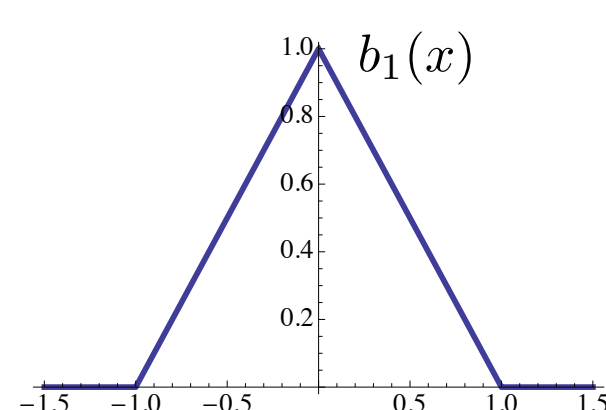
*



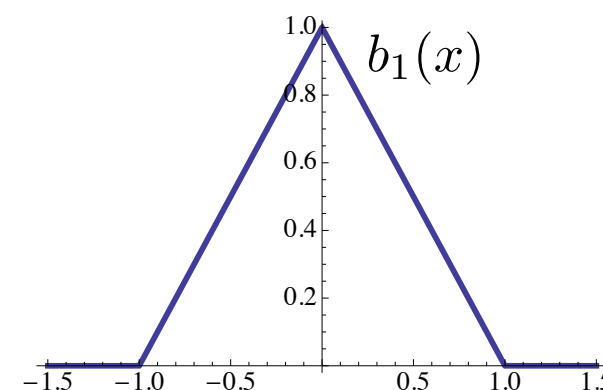
=



- For example, the cubic B-spline can be obtained in two different ways:



*



=

Dual Generators

- The box function is self-dual. Higher degree B-splines are not.
- Duals have the following Fourier-domain expression:

$$\hat{\hat{\varphi}}(\omega) = \frac{\hat{\varphi}(\omega)}{\hat{a}_{\varphi}(\omega)}$$

Dual Generators

- The box function is self-dual. Higher degree B-splines are not.
- Duals have the following Fourier-domain expression:

$$\hat{\hat{\varphi}}(\omega) = \frac{\hat{\varphi}(\omega)}{\hat{a}_{\varphi}(\omega)}$$

DTFT of the autocorrelation sequence.
Can be computed analytically for the B-splines.

Dual Generators

- The box function is self-dual. Higher degree B-splines are not.
- Duals have the following Fourier-domain expression:

$$\hat{\hat{\varphi}}(\omega) = \frac{\hat{\varphi}(\omega)}{\hat{a}_{\varphi}(\omega)}$$

DTFT of the autocorrelation sequence.
 Can be computed analytically for the B-splines.

- In the spatial domain:

$$\hat{\varphi}(x) = \sum_n a_{\varphi}^{-1}[n] \varphi(x - n)$$

Dual Generators

- The box function is self-dual. Higher degree B-splines are not.

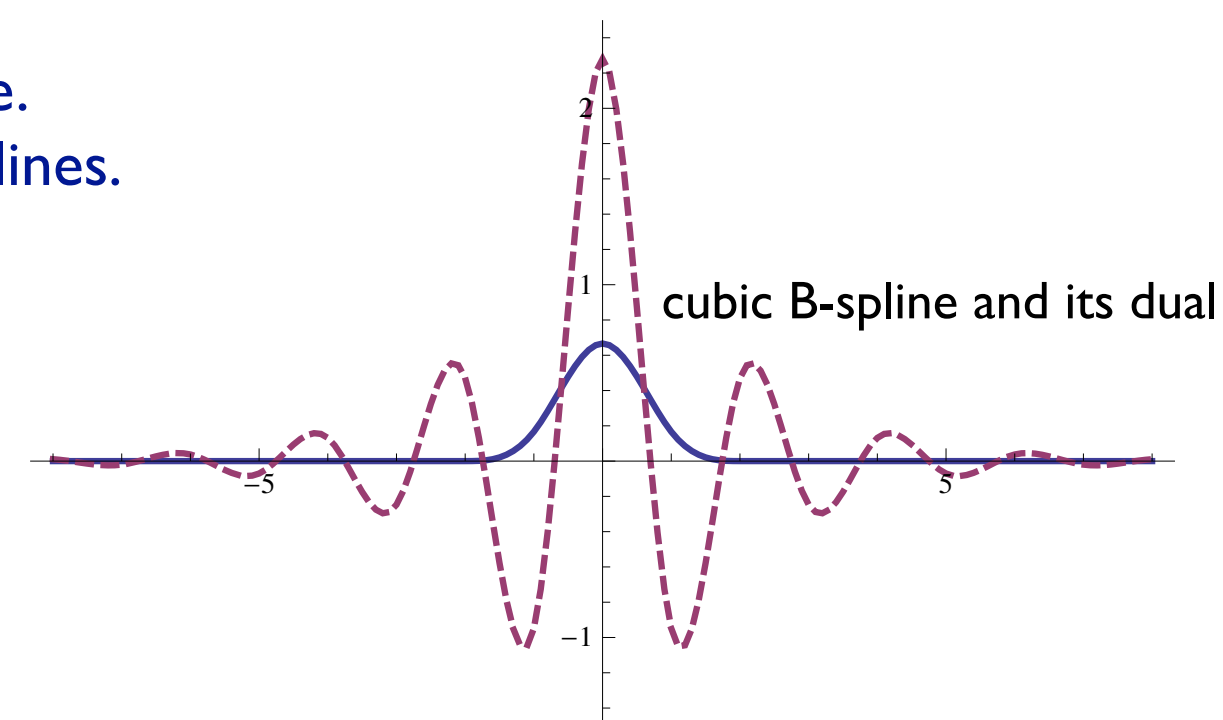
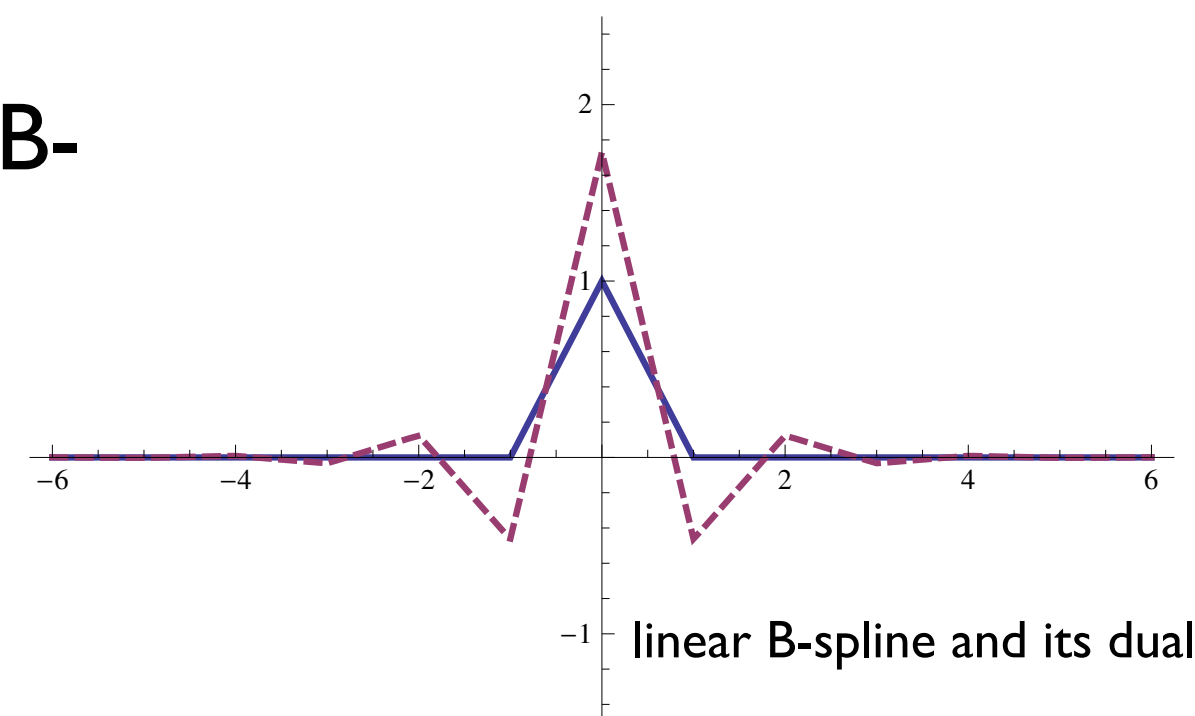
- Duals have the following Fourier-domain expression:

$$\hat{\hat{\varphi}}(\omega) = \frac{\hat{\varphi}(\omega)}{\hat{a}_{\varphi}(\omega)}$$

DTFT of the autocorrelation sequence.
 Can be computed analytically for the B-splines.

- In the spatial domain:

$$\hat{\varphi}(x) = \sum_n a_{\varphi}^{-1}[n] \varphi(x - n)$$



Rendering

- Recall that we wish to compute:

$$c[n] = \langle f, \dot{\varphi}(\cdot - n) \rangle$$

- Replacing the dual with its primal representation, we get:

$$\begin{aligned} c[n] &= \sum_m a_{\varphi}^{-1}[m] \langle f, \varphi(\cdot - (n - m)) \rangle \\ &= (r * a_{\varphi}^{-1})[n] \end{aligned}$$

Rendering

- Recall that we wish to compute:

$$c[n] = \langle f, \dot{\varphi}(\cdot - n) \rangle$$

- Replacing the dual with its primal representation, we get:

$$c[n] = \sum_m a_{\varphi}^{-1}[m] \langle f, \varphi(\cdot - (n - m)) \rangle$$

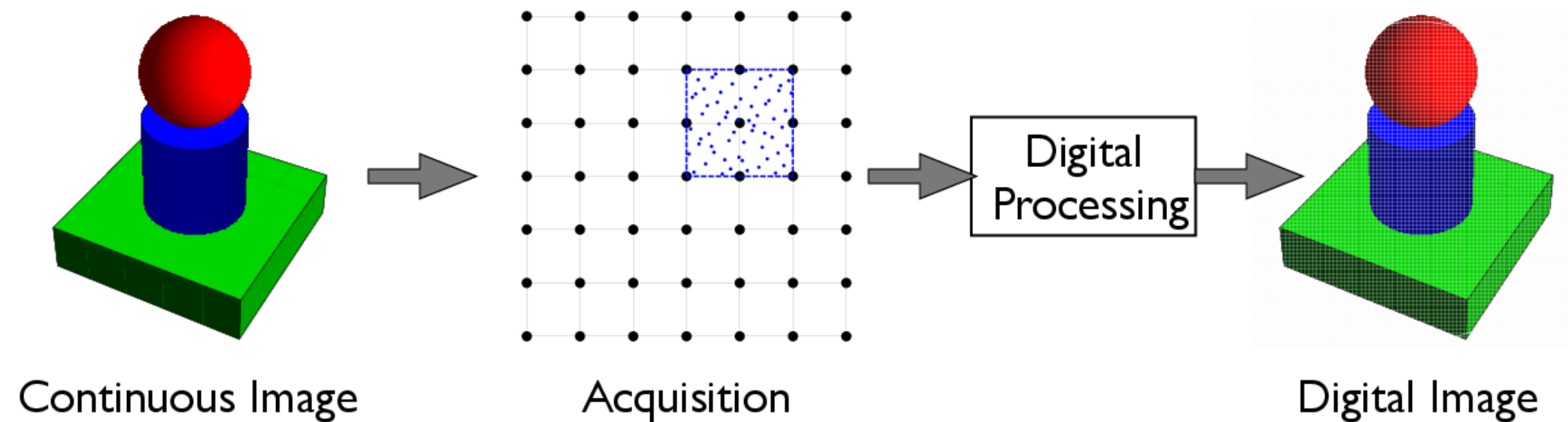
$$= (\underbrace{r}_{\text{analog acquisition}} * \underbrace{a_{\varphi}^{-1}}_{\text{digital processing}})[n]$$

analog acquisition

digital processing

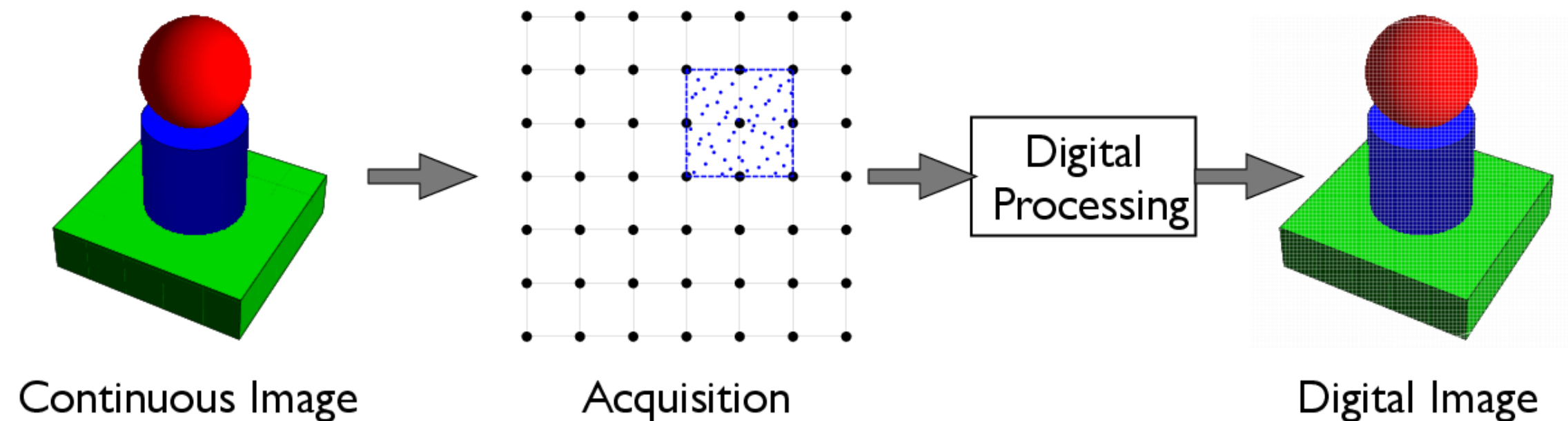
Rendering

$$f_{\text{app}}(x) = \sum_n (r * a_{\varphi}^{-1})[n] \varphi(x - n)$$



Rendering

$$f_{\text{app}}(x) = \sum_n (r * a_{\varphi}^{-1})[n] \varphi(x - n)$$

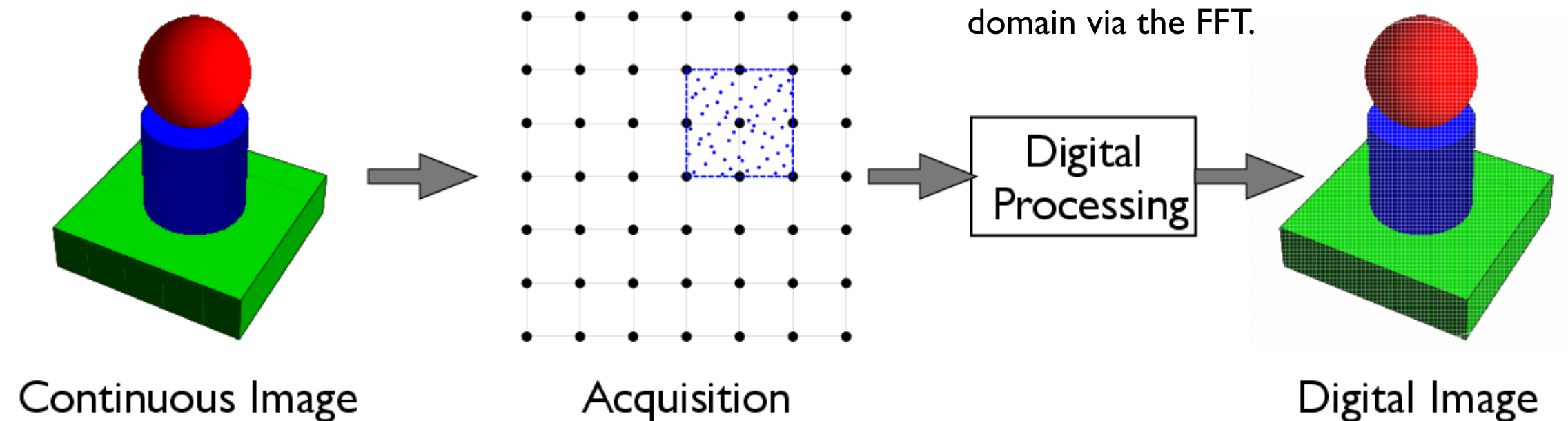


- Traces several rays through the support of the shifted generator.
- AKA antialiasing, smooths out high frequencies.

Rendering

$$f_{\text{app}}(x) = \sum_n (r * a_{\varphi}^{-1})[n] \varphi(x - n)$$

- Convolve with the inverse autocorrelation sequence.
- Restores some high frequencies.
- Efficiently implemented in the Fourier domain via the FFT.

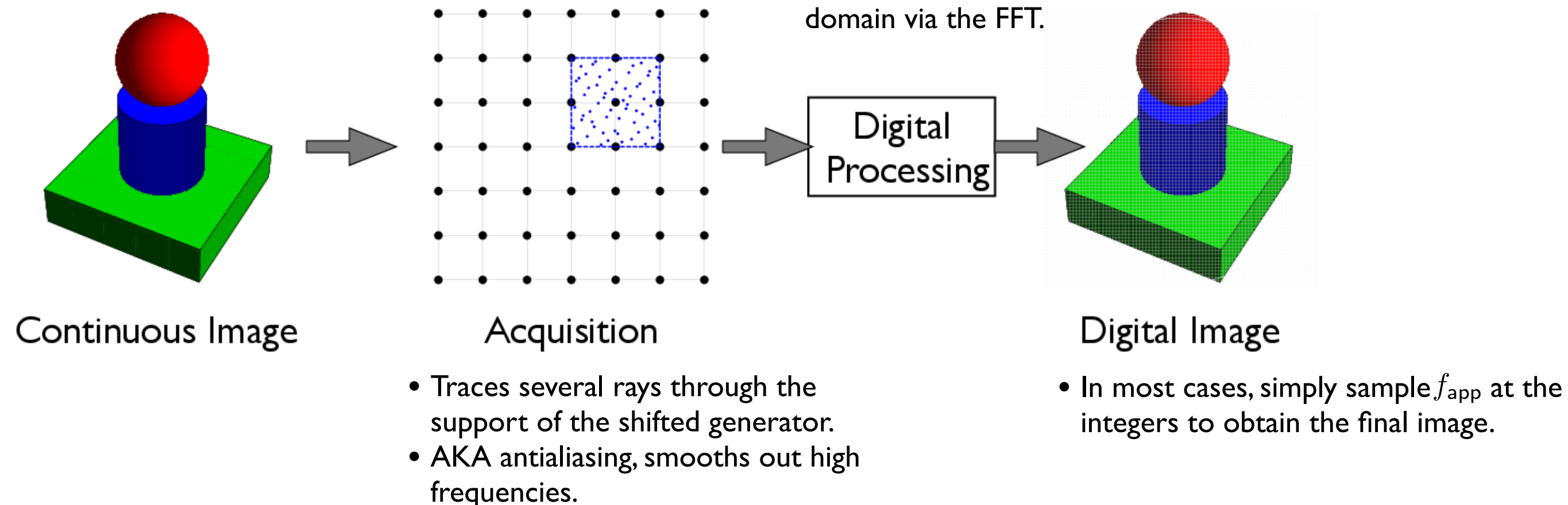


- Traces several rays through the support of the shifted generator.
- AKA antialiasing, smooths out high frequencies.

Rendering

$$f_{\text{app}}(x) = \sum_n (r * a_{\varphi}^{-1})[n] \varphi(x - n)$$

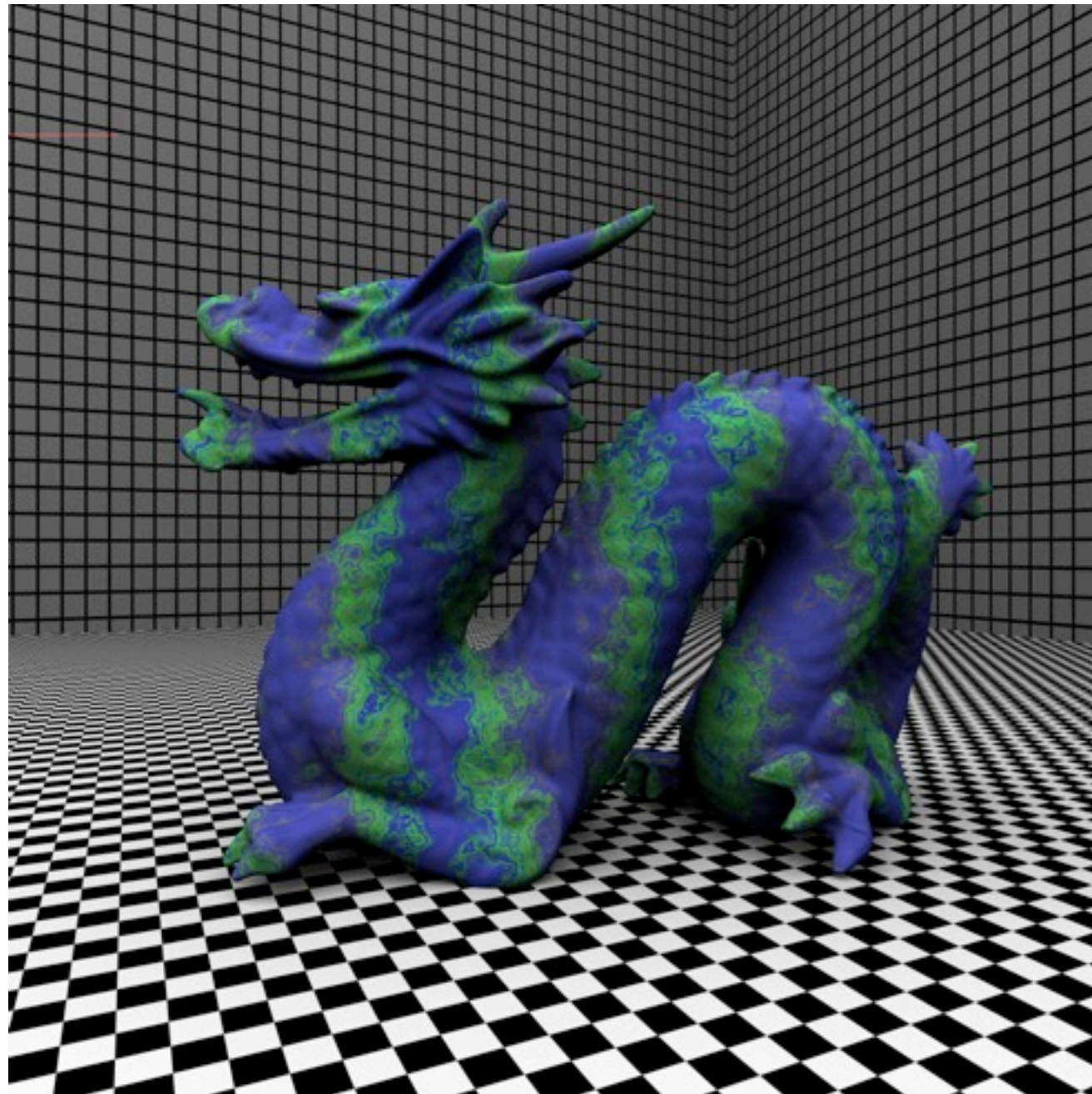
- Convolve with the inverse autocorrelation sequence.
- Restores some high frequencies.
- Efficiently implemented in the Fourier domain via the FFT.



Outline

- Motivation
- Shift-Invariant (SI) spaces
- Rendering in spaces generated by the uniform B-splines
- **Results**
- Conclusion

Test Scene



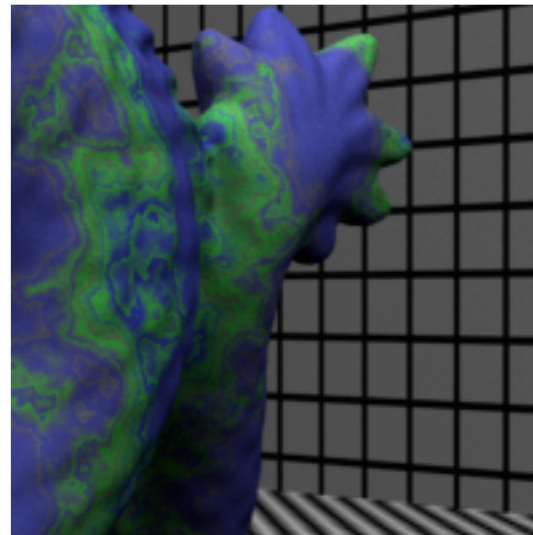
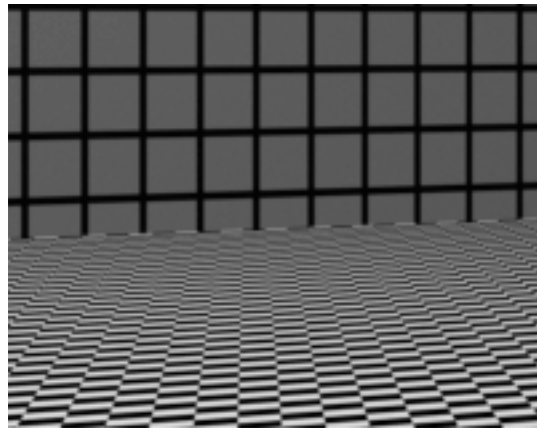
| Existing | OP |
|-----------------|------------------|
| conv. tent | min. error tent |
| MN | min. error cubic |

Experimental setup:

- Low discrepancy sampler (256 rays per coefficient)
- Rendered at a resolution of 1000 x 1000
- Low dynamic range

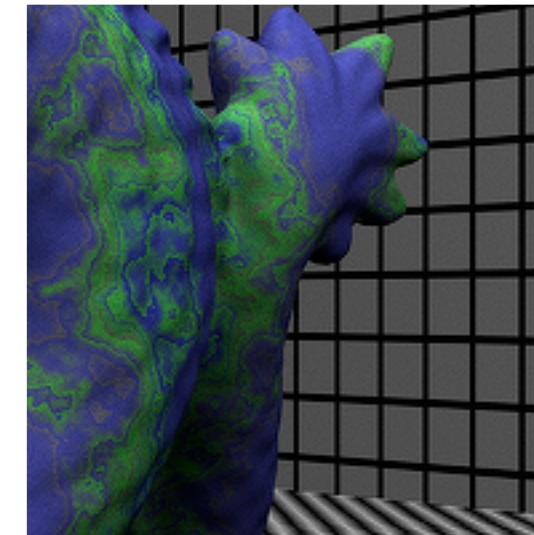
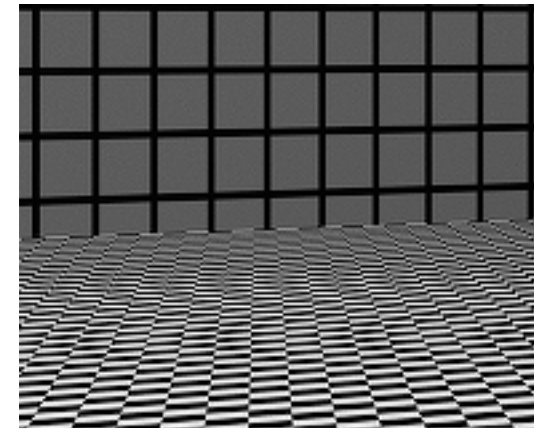
Linear Generators

conv. tent



- Effective anti-aliasing
- Smooths out detail in other areas

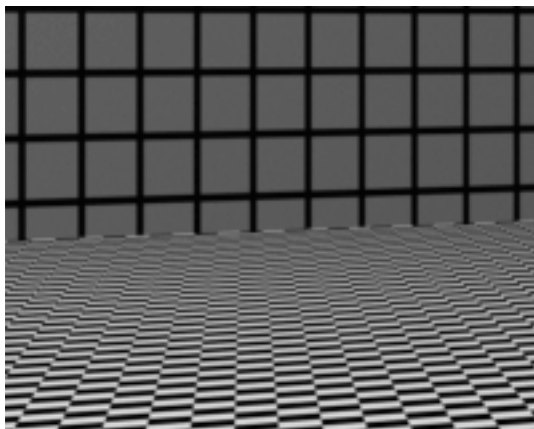
min. error tent



- Restores high frequency detail
- Introduces Moiré patterns

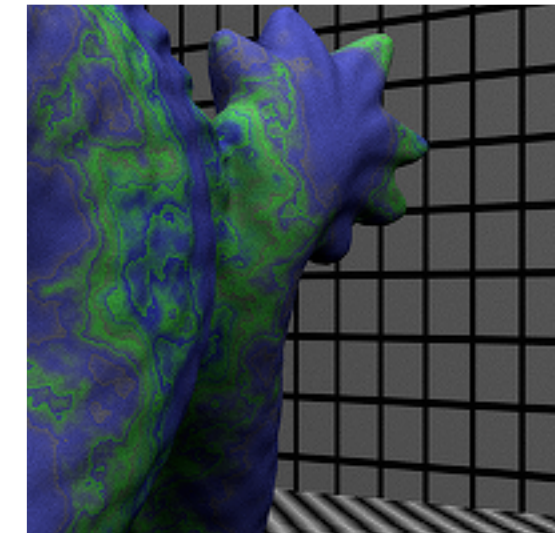
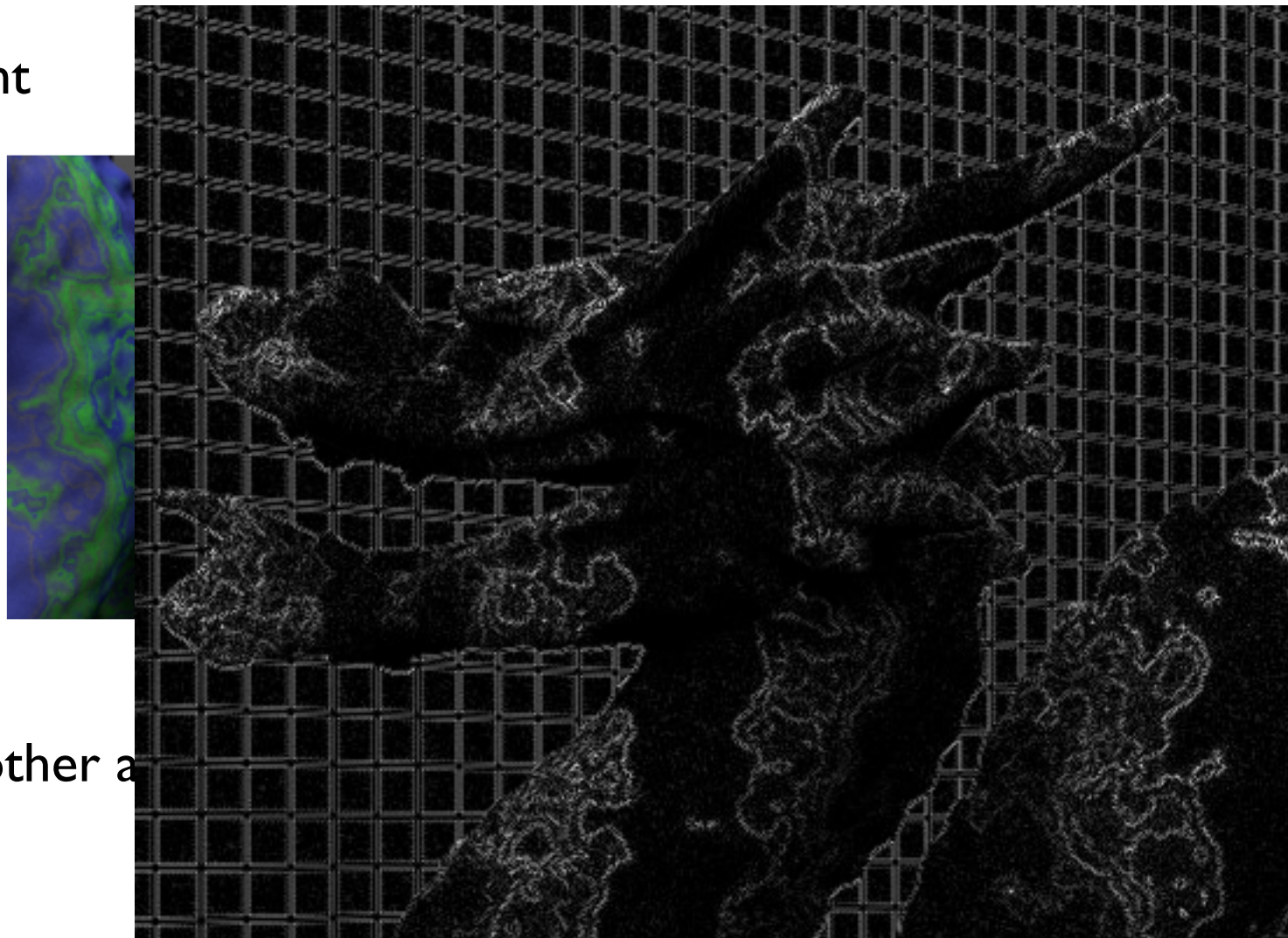
Linear Generators

conv. tent



- Effective anti-aliasing
- Smooths out detail in other areas

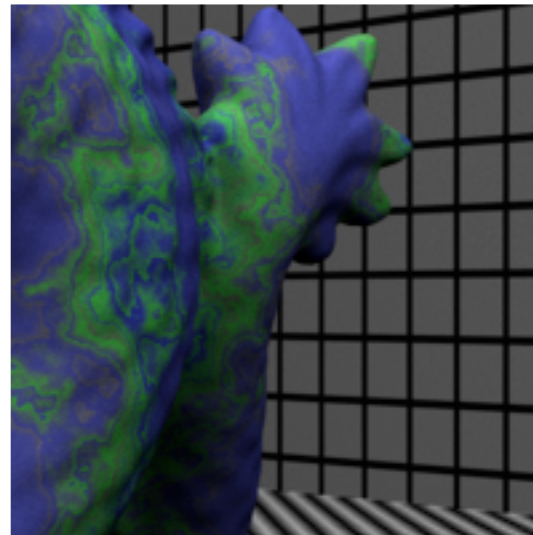
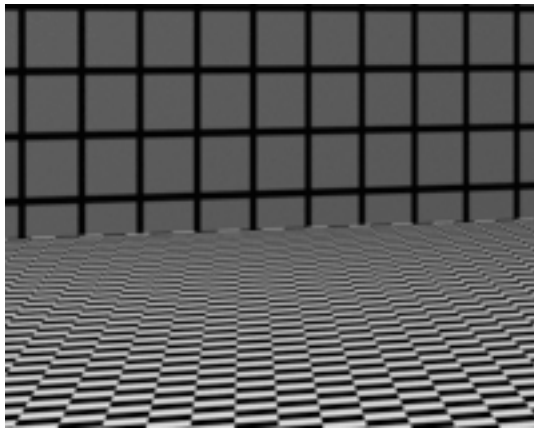
min. error tent


 frequency detail
 aliased patterns


difference image

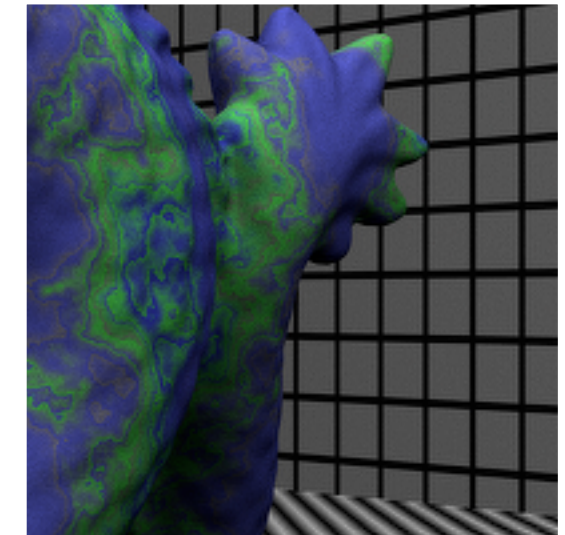
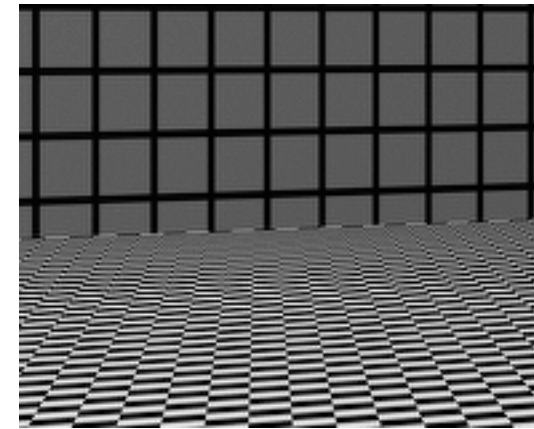
Cubic Generators

MN



- Effective anti-aliasing
- Slightly sharper than conv. tent

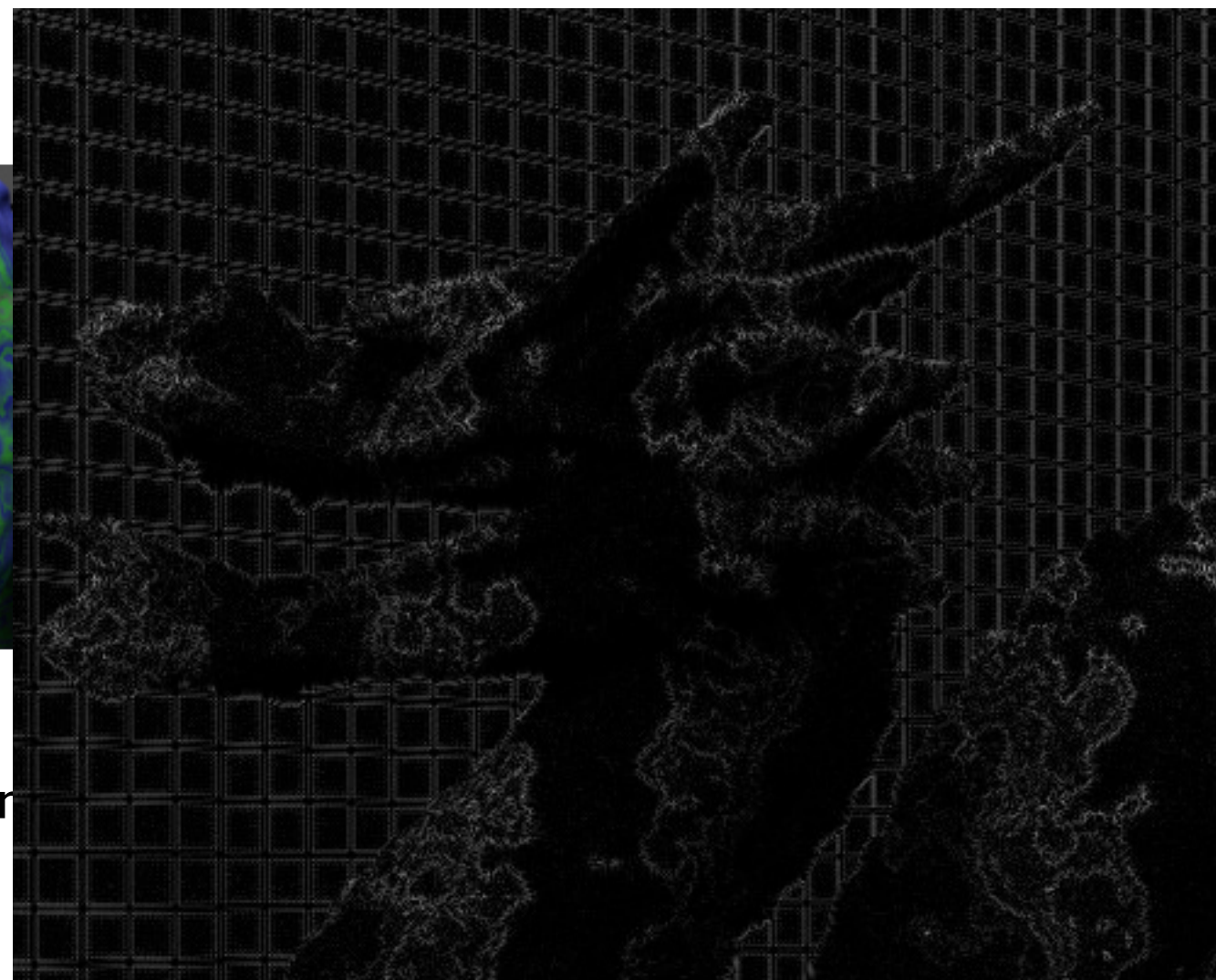
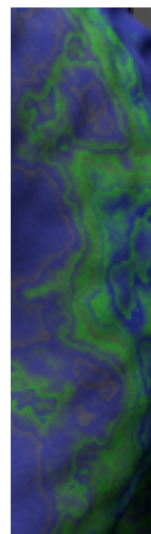
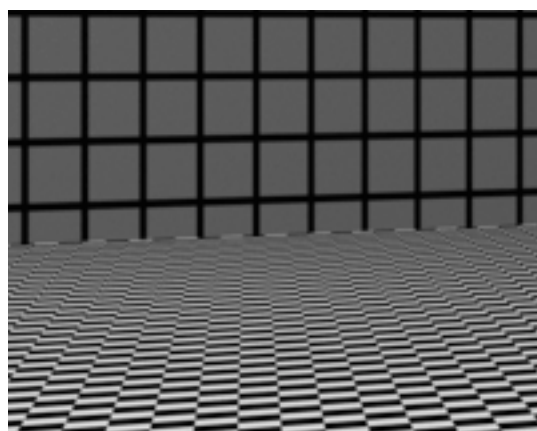
min. error cubic



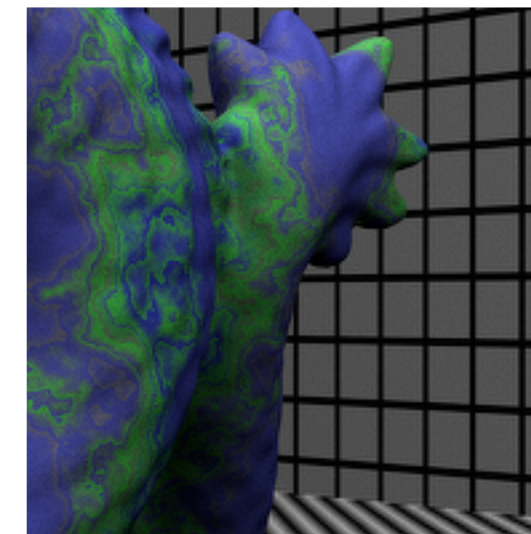
- Reduces Moiré patterns
- Slightly blurrier than min. error tent

Cubic Generators

MN



min. error cubic



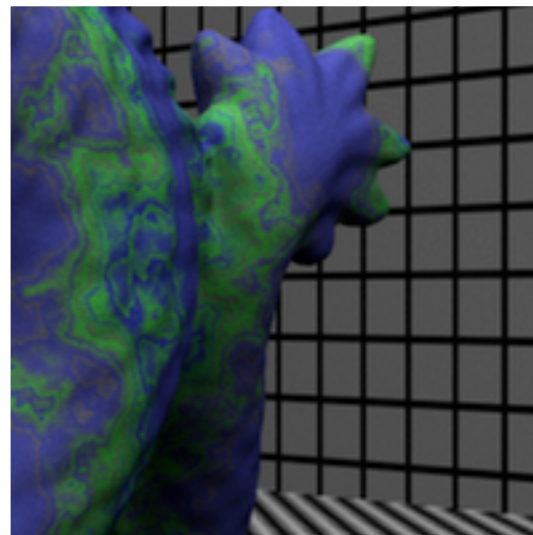
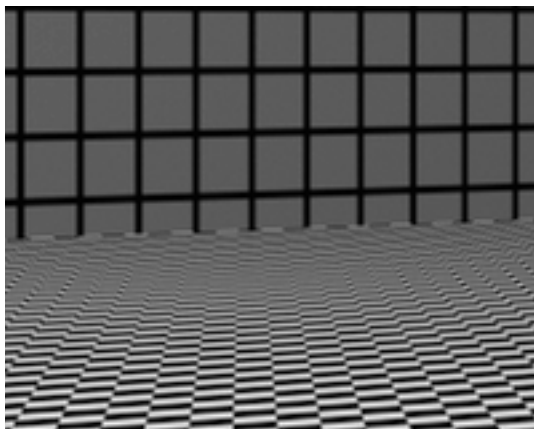
- Effective anti-aliasing
- Slightly sharper than conv. tent

patterns
than min. error tent

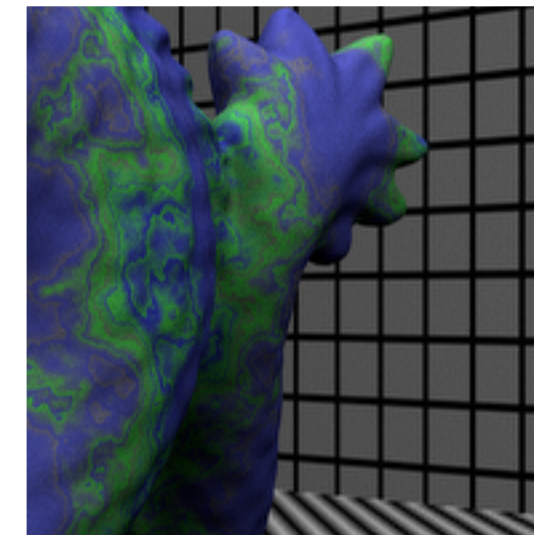
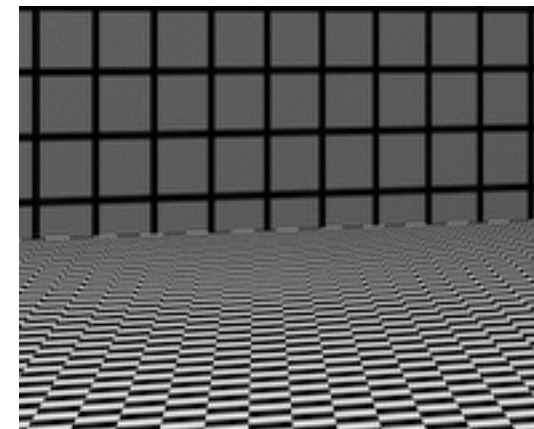
difference image

Removing Moiré Patterns

min. error tent



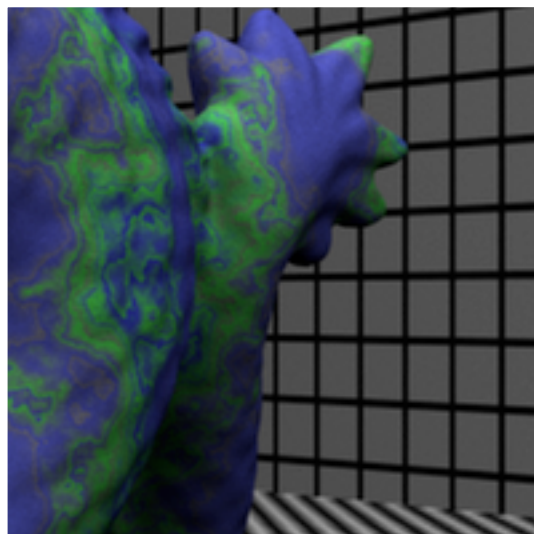
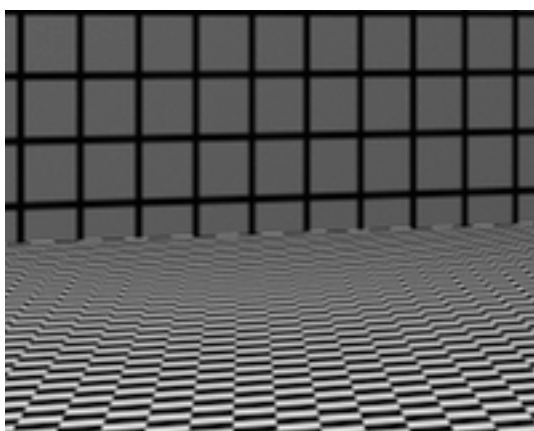
min. error cubic



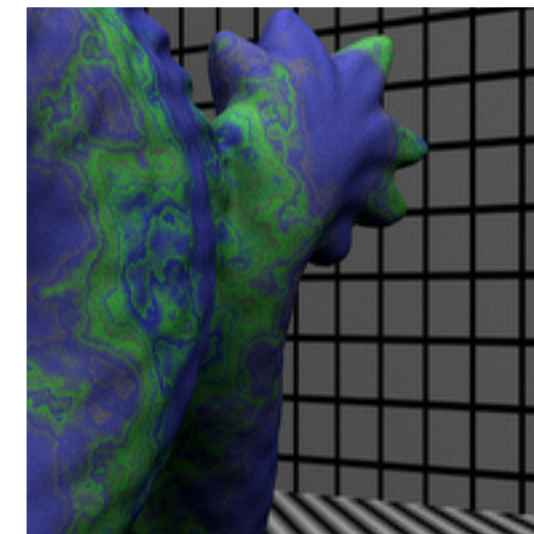
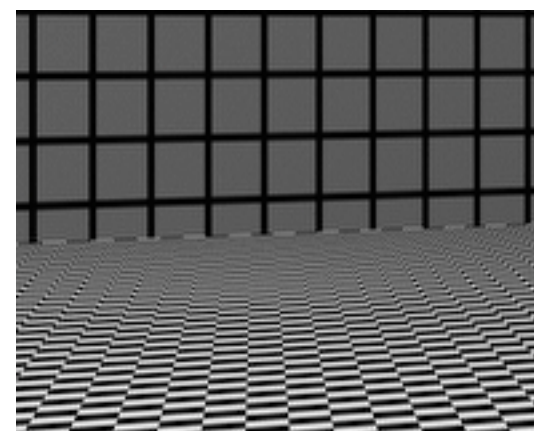
- Since $f_{\text{app}}(x)$ is continuous, it can be sampled at off-center points to diminish Moiré patterns.
- **Effective antialiasing without unduly sacrificing sharpness.**

Removing Moiré Patterns

min. error tent



min. error cubic



- Since $f_{\text{app}}(x)$ is continuous, it can be sampled at off-center points to diminish Moiré patterns.
- **Effective antialiasing without unduly sacrificing sharpness.**

| Filter | Percentage |
|----------------------|--------------|
| Box | 16.56 |
| Conv. tent | 15.19 |
| Min-error tent | 19.18 |
| Mitchell-Netravali | 15.50 |
| Min-error cubic | 17.41 |
| Min-error tent (AA) | 15.97 |
| Min-error cubic (AA) | 16.34 |

Energy percentage (measured via the FFT)
that lies in the high-pass regime

Not-so-synthetic Scenes

- Scenes that do not contain pathologically high frequencies have a clear advantage.



conv. tent



min. error tent

Not-so-synthetic Scenes

- Scenes that do not contain pathologically high frequencies have a clear advantage.



conv. tent

difference image

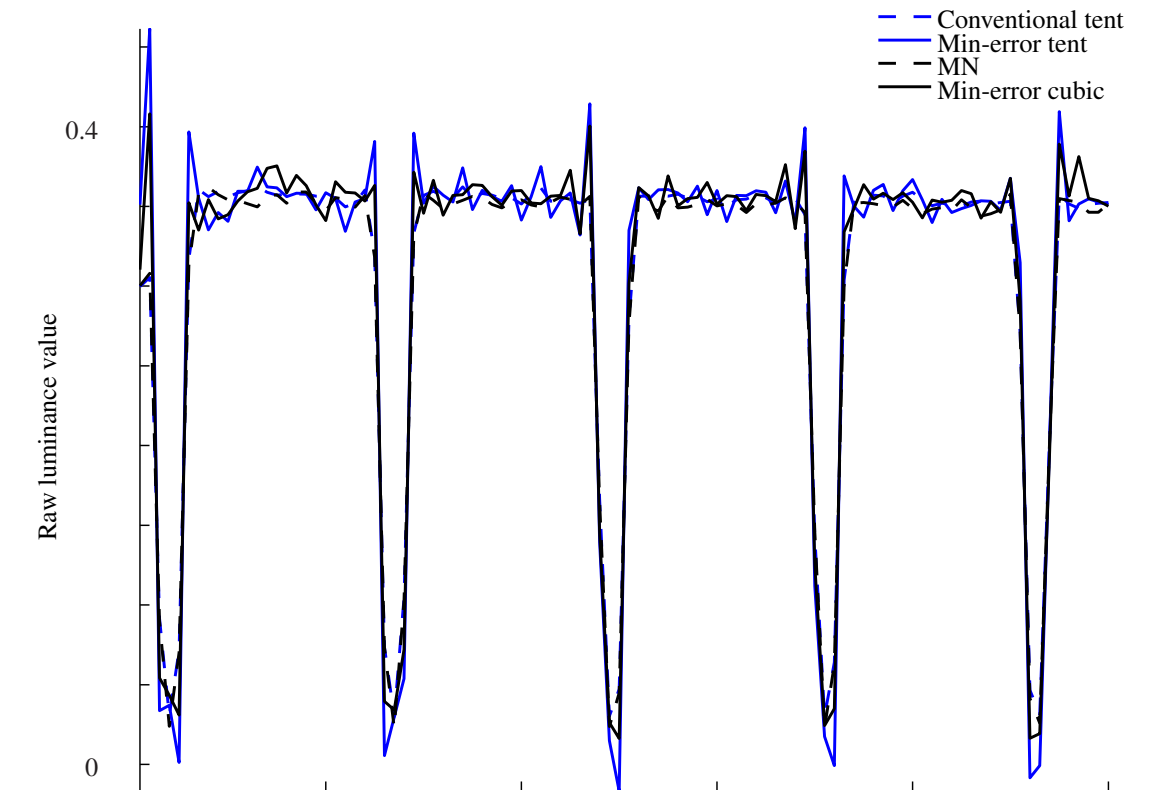
min. error tent

Outline

- Motivation
- Shift-Invariant (SI) spaces
- Rendering in spaces generated by the uniform B-splines
- Results
- **Conclusion**

Limitations

- Currently limited to LDR images. Further analysis is needed to extend to HDR images.
- Min. error approximation recovers high frequencies. Therefore, a relatively noise-free acquisition step is necessary.



Min. error approximation leads to overshoots and undershoots across discontinuities.

Future Work

- Extend to hexagonal grids, dynamic scenes
- Multiresolution
- Exploit sparsity, compressive sensing

Future Work

- Extend to hexagonal grids, dynamic scenes
- Multiresolution
- Exploit sparsity, compressive sensing

Thank you for your attention

ualim@ucalgary.ca

<http://visagg.cpsc.ucalgary.ca>